

Classical Advection of Guiding Centers in a Random Magnetic Field

L. Zielinski¹, K. Chaltikian¹, K. Bimbaum¹, C.M. Marcus¹, K. Campman² and A.C. Gossard²¹Department of Physics, Stanford University, Stanford, CA 94305-4060²Materials Department, University of California at Santa Barbara, Santa Barbara, CA 93106

(January 9, 2022)

We investigate theoretically and experimentally classical advective transport in a 2D electron gas in a random magnetic field. For uniform external perpendicular magnetic fields large compared to the random field we observe a strong enhancement of conductance compared to the ordinary Drude value. This can be understood as resulting from advection of cyclotron guiding centers. For low disorder this enhancement shows non-trivial scaling as a function of scattering time, with consistency between theory and experiment.

Transport in two-dimensional (2D) electron systems in a spatially random magnetic field (RMF) has generated great theoretical [1,8] and experimental interest [2,4,5] in recent years, and is now understood to be distinctly different from transport in systems with ordinary potential disorder. Experimentally, these systems have been realized using high-mobility heterostructure materials and overlayers of superconductors or ferromagnets [2,4,5] and may be related to quantum Hall transport around filling factor $\nu=2$ [1].

In the presence of a strong external uniform magnetic field and negligible potential disorder, electrons in a RMF move in spiraling cyclotron orbits with guiding centers moving along the contours of constant magnetic field [6]. Because contours are generically closed [17] electrons confined to contours do not contribute to total conductance in the limit of zero cyclotron radius. A similar situation arises in the case of electron gas moving in a long-range potential and strong uniform magnetic field, where the guiding centers move along the contours of constant potential, as recently discussed by Fogler et al. [7]. In that case, authors of [7] showed that a finite cyclotron radius allowing the electrons to "jump" between different contours only leads to an exponentially small conductance. In general, scattering from short-range potential disorder increases the probability of such jumps, significantly enhancing the conductance via the same mechanism: by freeing those electrons which would otherwise be trapped on closed contours of the RMF or long-range potential disorder. That type of transport may be called advective, in analogy with the well-studied problem in fluid dynamics where the transport of a tracer particle due to molecular diffusion becomes greatly enhanced due to the flow of the fluid [3].

A useful measure to analyze transport in a system with

both RMF and ordinary potential disorder is the ratio $R = \frac{\sigma_{RMF}}{\sigma_{xx}}$ of the longitudinal conductances with and without the RMF. In this Letter we present a novel analysis of advective transport in a RMF, leading to non-trivial scaling of the ratio R with the scattering time of the ordinary potential. We then compare theoretical predictions to experiments in a high-mobility 2D electron gas (2DEG) with a spatially random high-field magnet on the surface and controllable potential disorder.

We begin by discussing the classical statistical theory of electron motion in an inhomogeneous perpendicular magnetic field, $B(r)$. The following notation is used throughout the paper: $\langle \cdot \rangle$ and Δ represent respectively the average and standard deviation of the random cyclotron frequency $\omega_c(r) = \frac{eB(r)}{m^*c}$, ℓ_B and ℓ_P are the experimentally determined correlation lengths of the RMF and ordinary potential $V(r)$ respectively. The strengths and spatial scales of the two independent disorders relevant to the experiment satisfy the inequalities $\ell_P < v_F \max(\ell_0; \ell_1) < \ell_B, v_{ms} < E_F$, where v_F is the Fermi velocity and E_F is the Fermi energy, and it is these limits that we consider in this Letter. Note that the first inequality implies only that the random magnetic field varies slowly with position; no assumption about its strength is made.

To study transport in this mixed-disorder regime, we take advantage of the assumed separation of disorder length scales. Following the analysis of Ref. [8], magnetic randomness is treated as a Lorentz force term in the left hand side of the Boltzmann equation, while potential randomness leads to diffusion, characterized by a transport time τ_{tr} . Charge conservation then implies a diffusion equation for the fluctuating part of the particle density,

$$\frac{\partial n}{\partial t} = \frac{D_0}{1 + \frac{1}{2} r^2} r^2 \nabla^2 n + \frac{D_0}{1 + \frac{1}{2} r^2} \frac{1}{2 + 1} r^2 \nabla^2 n; \quad \frac{2}{2 + 1} r^2 \nabla^2 n; \quad (1)$$

where $\omega_c(r) = \omega_c(r) \tau_{tr}$ is the local dimensionless cyclotron parameter, $D_0 = \frac{1}{2} v_F^2 \tau_{tr}$ is the ordinary diffusion coefficient and $r^2 = (\partial/\partial y)^2$; $(\partial/\partial x)$ [9]. We will refer to the first and second terms in the r.h.s. as diffusive and advective terms respectively.

Equation (1) generalizes the standard advection-diffusion problem studied in fluid dynamics and plasma physics [17] described by the equation

$$\frac{\partial n}{\partial t} = D \nabla^2 n + u \cdot \nabla n \quad (2)$$

In the long-time, long-wavelength limit, solutions to Eq. (2) are known to converge to solutions of the usual diffusion equation [10,11],

$$\frac{\partial n}{\partial t} = D_e \nabla^2 n;$$

with an effective diffusion constant, D_e . In the standard advection-diffusion problem, Eq.(2), one distinguishes two regimes: the diffusive regime, in which the first (diffusive) term on the right hand side of Eq. (2) dominates and advection may be ignored, and the advective regime, in which the advective term makes a significant contribution to the transport coefficients. The dimensionless parameter characterizing the relative strength of advection over diffusion is the so-called Peclet number $P = u_0/D$, where u_0 and D are respectively the characteristic spatial scale and amplitude of the random velocity field $u(r)$.

Now, returning to our problem, Eq. (1), the Peclet number in this case is approximately given by the RMF cyclotron parameter, $P = \tau_{tr} \omega_c$ and the two corresponding transport regimes are defined as follows:

(i) Strong disorder, when the inequality $\tau_{tr} \omega_c \ll 1$ is obeyed. This corresponds to the diffusive regime. Here the advective term is negligible and the effective diffusion constant is approximated by $D_e = D_0 \frac{1}{1 + \tau_{tr}^2}$:

(ii) Weak disorder and strong magnetic field, when the inequality $\tau_{tr} \omega_c \gg 1$ is obeyed. This corresponds to the advective regime. In this regime Eq.(1) is well approximated by the form of Eq. (2) with $D = D_0 \frac{1}{1 + \tau_{tr}^2}$ and $u = D \nabla \varphi$. The dependence of D_e on the bare diffusion constant D in this regime, characterized by large Peclet numbers, ($P \gg 1$) has been a subject of several theoretical and numerical studies over the past decade [12,14[17]. Heuristic arguments [14] and non-local variational principles [16] lead to the expression $D_e = D a(\tau_{tr}) P^{-\alpha}$, where $a(\tau_{tr}) = \frac{1 + (\tau_{tr} \omega_c)^2}{(\tau_{tr} \omega_c)^2 + (\tau_{tr} \omega_c)^2}$ [9]. In the limit $\tau_{tr} \omega_c \gg 1$, the prefactor $a(\tau_{tr}) \rightarrow 1$, giving the simple scaling form

$$D_e = D P^{-\alpha}; \quad (3)$$

where

$$\alpha = \frac{1 + d_f}{2 + d_f} \quad (4)$$

is a constant that depends on the geometry and statistical properties of the random surface. In Eq.(4), α is the critical exponent for the correlation length of the level contours of $B(r)$, and d_f is the fractal dimension of these contours [17]. If $B(r)$ has Gaussian statistics and is short-range correlated, then $\alpha = \frac{4}{3}$ and $d_f = \frac{7}{4}$ [18],

giving $\alpha = \frac{10}{13} \approx 0.77$ [14]. For non-Gaussian statistics of $B(r)$, the value of α depends on the distribution of saddle-point heights [19]. If $B(r)$ is doubly periodic, for instance, then $\alpha = d_f = 0$, giving $\alpha = \frac{1}{2}$, a result known from boundary layer considerations [13]. The scaling relation, Eq.(3), is the main signature of advective transport that we investigate experimentally, as described below. The experimental system consists of a 200 nm wide

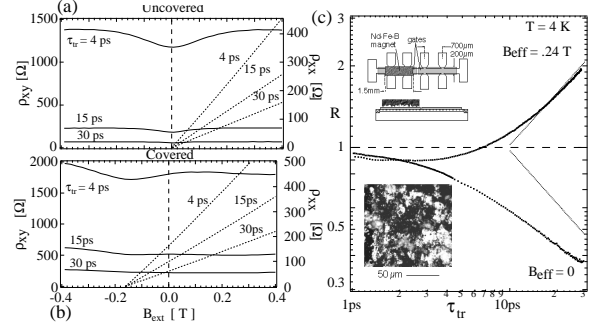


FIG. 1. (a) Hall (left axis) and longitudinal (right axis) resistivities for the uncovered half of the Hall bar at three different values of τ_{tr} vs. external magnetic field, B_{ext} . Note that for the uncovered half $B_e = B_{ext}$. (b) Corresponding graphs for the covered half. Note the shift of the effective magnetic field, $B_e = B_{ext} - 0.15T$. Zero of B_e is by definition the point of intersection of Hall slopes. (c) The ratio $R = \frac{R_{xx}^{RMF}}{R_{xx}}$ plotted for two representative values of B_e showing the suppression of the RMF conductance at $B_e = 0$ and the strong enhancement due to advection at high field. Dotted lines show the theoretical expression $R = a(\tau_{tr}) P^{-\alpha}$. In the limit $\tau_{tr} \gg 1$, $R = P^{-\alpha}$ in the advective regime ($B_e = 0.24T$) and $R = P^{-\alpha}$ in the diffusive regime ($B_e = 0$). In both cases the values $\alpha = 0.65$ and $B_{rms} = 0.04T$ giving the best fit were used. Upper inset: Schematic of the device, including gates and attached magnet. Lower inset: Optical micrograph of the Nd-Fe-B surface indicating roughness on the 20 nm scale.

by 3 nm long Hall bar fabricated from a high-mobility GaS/AlGaS heterostructure (see Fig. 1c, inset). Sheet density and scattering times are controlled by applying voltages in the range $V_{gate} = -1.2$ to $+0.7V$ via two independent gates thermally evaporated onto one half of each structure (gate material is 100 Å Cr followed by 2500 Å Au). To generate the random magnetic field, a neodymium-iron-boron (Nd-Fe-B) permanent magnet (300 nm wide, 200 nm tall, 1.5 mm long) was sixed with polymethylmethacrylate (PMMA) to the Hall bar above the gate with the easy magnetization axis of the sintered material perpendicular to the surface [4,5]. The Nd-Fe-B magnet is attached in a demagnetized state, but after cooling the sample and ramping an external perpendicular magnetic field B_{ext} to 6T, the material becomes permanently magnetized, creating a field of $B_0 = 0.15T$ at the electron gas measured from the Hall resistance o -

set, seen as the intersection point of the Hall resistances in Fig. 1b. The effective average field B_e felt by the electrons is the difference between the applied field and this constant offset, $B_e = B_{\text{ext}} - B_0$.

The rough surface of the Nd-Fe-B (Fig. 1c, lower inset) generates a spatially random magnetic field at the 2DEG with standard deviation $B = 0.04\text{T}$ (measured by a best fit low-field magnetoresistance [4]), and characteristic length scale $B = 20\text{m}$. The permament magnetization is insensitive to changes in B_{ext} in the range 0.5T to 0.5T of interest in the experiment, and little hysteresis is observed in this range following initial magnetization. Longitudinal and Hall resistances were measured at 4.2K on both the end of the Hall bar under the magnet ("covered") and the end without the magnet ("uncovered") using standard lock-in techniques at 3Hz with a current bias of 100nA . Following the transport measurements in the RMF, the Nd-Fe-B magnet was taken off and the measurements repeated on the previously covered side. We note that at these temperatures and magnetic fields quantum effects in the form of Shubnikov-deHaas oscillations are not observed [5]. Conductivities with and without the RMF, R_{xx}^{RMF} and R_{xx} , were then computed from the measured R_{xx} 's and R_{xy} 's as a function of gate voltage. The non-RMF data are based on the runs after removing the magnet, with the uncovered half of the sample serving as a control. The dependence of τ_{tr} on V_{gate} was found to be repeatable for a particular sample through multiple thermocyclings, allowing V_{gate} to serve as a reliable and repeatable 'knob' controlling τ_{tr} .

Two samples with different ranges of transport elastic scattering time $\tau_{\text{tr}}(V_{\text{gate}})$ are reported. In sample 1, τ_{tr} ranged from 0.1 to 10ps , corresponding to ranges $n = 7.9 \cdot 10^5$ to $1.2 \cdot 10^6\text{m}^{-2}$ and $\mu = 0.23$ to $26\text{m}^2/\text{Vs}$. In sample 2, τ_{tr} ranged from 0.5 to 30ps , corresponding to ranges $n = 9.9 \cdot 10^4$ to $3.8 \cdot 10^5\text{cm}^{-2}$ and $\mu = 2.2$ to $78\text{m}^2/\text{Vs}$. We will concentrate on data from the "cleaner" sample 2 since the advective regime is reached more easily for larger τ_{tr} . Figure 1c shows the ratio $R = \frac{R_{xx}^{\text{RMF}}}{R_{xx}}$ as a function of τ_{tr} at effective magnetic field $B_e = 0$ and $B_e = 0.24\text{T}$. The ratio R is equivalent to the ratio $D_e = D$ and so is expected to scale with τ_{tr} as in Eq. (3) in the advective regime. Figure 1c illustrates the key difference between the advective and diffusive regimes: At low B_e (the diffusive regime) the RMF acts to increase the total disorder, so that as τ_{tr} is increased (potential scattering reduced), the RMF becomes the dominant source of scattering, leading to a decreasing R with increasing τ_{tr} . On the other hand, for larger B_e the advective regime is reached and the RMF causes advection of guiding centers, leading to an increasing R with increasing τ_{tr} , as predicted by Eq. (3). Figure 2 shows in greater detail how this transition from the diffusive to the advective regime depends on B_e . The transition is indicated by a crossover from decreasing to increasing R with increasing τ_{tr} , marked by

a triangle below each trace in Fig. 2. For higher B_e the crossover region moves to lower values of τ_{tr} with the minimum of R ($\tau_{\text{tr}, \text{min}}$) depending on B_e , according to $\tau_{\text{tr}, \text{min}} \propto B_e^{-1}$ (see Fig. 2, inset). To look for scaling in the

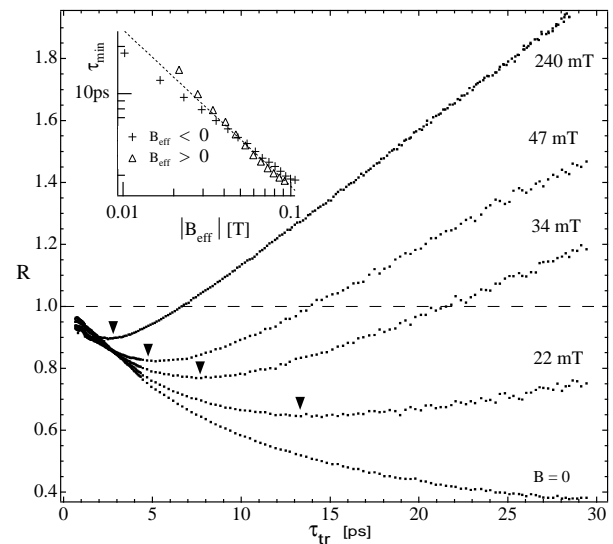


FIG. 2. The ratio $R = \frac{R_{xx}^{\text{RMF}}}{R_{xx}}$ measured at different values of B_e showing the gradual shift of the transition region between the diffusive and the advective regimes with increasing B_e . The location of the minimum of R , $\tau_{\text{tr}, \text{min}}$, indicated by triangles, is plotted in the inset as a function of B_e showing a power law dependence $\tau_{\text{tr}, \text{min}} \propto B_e^{-1}$.

advective regime, $\tau_{\text{tr}} > \tau_{\text{tr}, \text{min}}$, we define a scaling exponent

$$(B_e; \tau_{\text{tr}}) = \frac{d \ln(R)}{d \ln(\tau_{\text{tr}})} \quad (5)$$

comparable to β in Eq. (3). Figure 3 shows the measured R as a function of τ_{tr} at different values of B_e and in the inset as a function of B_e at fixed τ_{tr} . We see that only for $B_e = 0$ (in the high-mobility sample for $B_e < 0.01\text{T}$) does R remain negative for all values of τ_{tr} . This behavior indicates that R decreases monotonically around $B_e = 0$ as already seen in Fig. 1c). As we increase B_e , R levels off for large values of τ_{tr} , which we interpret as having entered the advective regime of (3). A characteristic feature of R as a function of B_e (inset, Fig. 3) is the dip near zero that becomes deeper for larger τ_{tr} . This is expected from our prediction that $(0; \tau_{\text{tr}})$ should be monotonically decreasing with increasing τ_{tr} .

Figure 3 indicates that the advective regime is first reached at $\tau_{\text{tr}} = 22\text{ps}$ ($\mu = 5.72$), at high magnetic fields, where $(B_e; 22\text{ps}) \approx 0.65$. The $\tau_{\text{tr}} = 22\text{ps}$ data, shown as the topmost curve in the inset of Fig. 3, emphasizes the asymptotic nature of the evolution of R . At higher τ_{tr} , for $B_e > 0.1\text{T}$, $(B_e; \tau_{\text{tr}})$ is virtually constant at 0.65 . This constant value of β , independent of τ_{tr} and

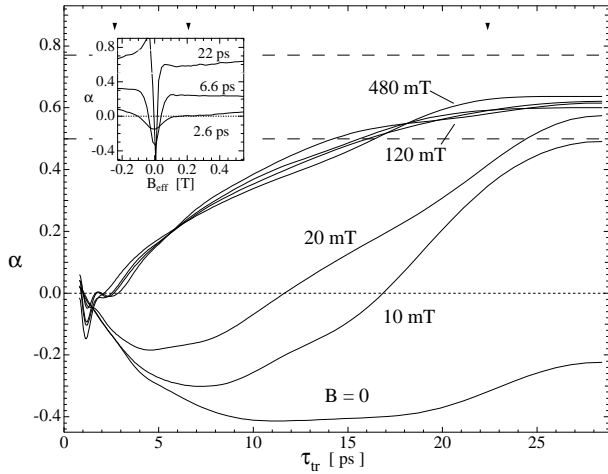


FIG. 3. Scaling exponent $\alpha = d \ln(R) = d \ln(\tau_{tr})$ as a function of τ_{tr} at different values of B_e . The saturation at 0.65 for $B_e > 120$ mT and $\tau_{tr} > 20$ ps is a signature of the advective regime and corresponds to a power law R / τ_{tr} . The two horizontal dashed lines correspond to the two limiting cases of periodic ($\alpha = 0.5$) and gaussian disordered $B(r)$ ($\alpha = 0.77$). One expects $0.5 < \alpha < 0.77$ for any physical system. Inset shows α as a function of B_e at three values of τ_{tr} (marked by filled triangles in the main figure). The topmost curve at $\tau_{tr} = 22$ ps asymptotically approaches 0.65 for high values of B_e . For larger values of τ_{tr} , remains constant at 0.65 for $B_e > 0.1$ T.

B_e is the experimental signature of the expected power law, R / τ_{tr} . The measured scaling exponent $\alpha = 0.65$ is within the range $1=2 < \alpha < 10=13$ expected from the present theory. The specific attributes of the experiment which lead to the particular value 0.65 are not understood at this point, however it is known that deviations from gaussian fluctuations of $B(r)$ will change the scaling of advective transport within the range allowed by Eq. (4).

In summary, we have investigated classical advection of guiding center motion of disordered 2DEG in a RMF, and found theoretically a novel scaling of the ratio R of diffusion constants or conductivities with and without the RMF as a function of τ_{tr} . Experiments confirm the expected power law scaling, and give a scaling exponent consistent with theory.

We thank S.C. Zhang and G.C. Papanicolaou for useful discussion. We acknowledge support at Stanford from the ONR under Grant N00014-94-1-0622, the Army Research Office under grant DAAH04-95-1-0331, the NSF-NYI program (C.M.M.), the NSF under grant DMR-9522915 (K.C.), the NSF Center for Materials Research, and the URO program (L.Z.) and Teran Fellowship at Stanford. We also acknowledge support at UCSB by the AFOSR under Grant F49620-94-1-0158 and QUEST.

- [1] V. Kalneyer and S. C. Zhang, Phys. Rev. B 46, 9889 (1992); B. I. Halperin, P. A. Lee and N. Read, Phys. Rev. B 47, 7312 (1993); V. Kalneyer, D. Wei, D. Arovas and S. C. Zhang, Phys. Rev. B 48, 11095 (1993); B. L. Altshuler and L. B. Ioje, Phys. Rev. Lett. 69, 2979 (1992); D. V. Khveshchenko and S. V. Meshkov, Phys. Rev. B 47, 12051 (1993); A. G. Aronov, A. D. Mirlin and P. Wolke, Phys. Rev. B 49, 16609 (1994); K. Chaltikian, L. Pryadko and S. C. Zhang, Phys. Rev. B 52, R8688 (1995); A. D. Mirlin, E. A. Itshuler and P. Wolke, Annalen der Physik 5, 281 (1996).
- [2] A. Geim, S. Bending and I. Grigorieva, Phys. Rev. Lett. 69, 2252 (1992); A. Smith et al., Surface Science 361-362, 349 (1996); A. Nogaret et al., University of Nottingham preprint (1997).
- [3] T. E. Taber, Fluid Dynamics for Physicists (Cambridge University Press, 1995).
- [4] F. B. Manco et al. Phys. Rev. B 51, 13269 (1995).
- [5] F. B. Manco et al. Phys. Rev. B 53, R7599 (1996).
- [6] T. G. Northrop, The Adiabatic Motion of Charged Particles, (New York, Interscience Publishers, 1963).
- [7] M. M. Fogler, A. Yu. Dobin, V. I. Perel, and B. I. Shklovskii, Phys. Rev. B 56, 6823 (1997).
- [8] P. Hedegard and A. Smith, Phys. Rev. B 51, 10869 (1995).
- [9] K. Chaltikian, Ph.D. Thesis, Stanford University (1997).
- [10] G. C. Papanicolaou and S. Varadhan, in: Boundary Value problems with rapidly oscillating random coefficients, (North Holland, Amsterdam, 1982), 835.
- [11] D. M. Laughlin, G. C. Papanicolaou and O. Pironneau, SIAM J. Appl. Math. 45, 780 (1985).
- [12] Yu. A. Dreizin and A. M. Dykhne, Sov. Phys. JETP 36, 127 (1973).
- [13] S. Childress, Phys. Earth Planet Int. 20, 172 (1979).
- [14] M. B. Isichenko et al., Sov. Phys. JETP 69, 517 (1989).
- [15] M. Avellaneda and A. J. Majda, Comm. Math. Phys. 138, 339 (1991).
- [16] A. Fanjiang and G. C. Papanicolaou, Stanford University preprint (1996).
- [17] M. B. Isichenko, Rev. Mod. Phys. 64, 961 (1992).
- [18] H. Saleur and B. Duplantier, Phys. Rev. Lett. 58, 2325 (1987).
- [19] If the probability to have a saddle point at a level in the interval $[B; B + dB]$ is given by $dP(B) = B^{-1} dB$ at small B , then $\alpha = \frac{4}{3}(\alpha + 1)$.